Research Journal of Chemical Sciences ISSN 2231-606X
Vol. **7(5),** 46-58, May **(2017)** *Res. J. Chem. Sci.*

A comparison of the Minnesota family of density functionals for the calculation of conceptual DFT descriptors: citrus flavonoids as a test case

Juan Frau[1], Francisco Muñoz[1] and Daniel Glossman-Mitnik[1,2,*]
[1]Departament de Química, Universitat de les Illes Balears, 07122 Palma de Mallorca, Spain
[2]Laboratorio Virtual NANOCOSMOS, Departamento de Medio Ambiente y Energía, Centro de Investigación en Materiales Avanzados, Chihuahua, Chih 31136, Mexico
daniel.glossman@cimav.edu.mx

Available online at: www.isca.in, www.isca.me
Received 22nd March 2017, revised 5th May 2017, accepted 14th May 2017

Abstract

This study illustrates the assessment of the Minnesota family of density functionals usefulness in calculating the properties and structure of molecular systems consisting of three citrus flavonoids molecules with potential to inhibit the nonenzymatic glycation of amino acids and proteins and considered antioxidants for avoiding the action of metallic ions, like Cu, Al and Fe. Conceptual DFT is used in calculating the chemical reactivity descriptors and active sites for nucleophilic and electrophilic attacks chosen by linking them to Fukui function indices, the condensed local hypersoftness (LHS) and the dual descriptor$\Delta f(r)$. The accuracy of the studied density functionals alongside their validity is checked by comparing their results in descriptors calculated using vertical energy values with the HOMO and LUMO results derived from Koopmans' theorem approximation.

Keywords: Computational Chemistry, Molecular Modeling, Natural Products, Hesperetin, Hesperidin, Neohesperidin, Conceptual DFT, Chemical Reactivity Theory.

Introduction

Conceptual Density Functional Theory (CDFT) identified popularly as Chemical Reactivity Theory forms a useful tool in predicting, analyzing, and interpreting possible results of chemical reactions[1-4]. Knowing reactivity occurring on molecules is an important for enabling in-depth understanding of interactions involved in every reaction mechanism. Specifically, the knowledge of reactivity has proved crucial in explaining electrostatic interactions from using the molecular electrostatic potential[5,6].

The use of Conceptual DFT has facilitated rationalizing reaction mechanisms with a desire to quantify and gain deeper knowledge on covalent interactions. Rationalizing reaction mechanisms of electrophilic regions from overlaps found in electrophilic regions to optimize stabilization translates to intermediates and final products.

Allied to the Parr breakthrough[1], his pioneer work has become a vital source of several concepts developed from analyzing densities of various molecular using the DFT. The derived concepts enable researchers in making qualitative predictions from understanding the chemical reactivity occurring in a particular system. Additionally, the concepts support the conceptual DFT descriptors identified as quantifying chemical reactivity.

The use Chemical Reactivity Theory in generating quantitative values obligate applying the Kohn-Sham theory while calculating the molecular densities. Besides generating values for the Conceptual DFT Descriptors, Kohn-Sham theory supports calculations for system energy and orbital energies. This is crucial for energies attributed to the frontier orbital - HOMO and LUMO[7-12].

Choosing the model chemistry forms the initial stage for studying molecular system and desired chemical reaction. Here, a model chemistry involves a collection of density functional, implicit solvent and basis set model considered sufficient for the studied problem. Literature offers an extensive list of various ways of choosing model chemistry. A significant number of them embrace documents experience of previous researchers. Nevertheless, the chosen model chemistry would vary relative to the nature of the task studied.

While the framework of DFT emphasizes the existence of a universal density functional and ability to derive all system properties by calculating using the functional, approximate density functional are equally useful in practice. As such, the frequently used approximate density functional developed in the last three decades. Since they are approximating functional in nature, their prediction suitability varies across properties unlike the universal functional. For instance, they offer excellent description of properties evident in specific molecular system and functional group. This necessitates using other density functional from multiple functional group that fit the studied molecular system.

Besides ground state, performing calculations for open systems such as radical cation and anion is important in studying chemical reactivity involving electrons transfer. The nature of the processes involved, makes the systems challenging to accomplish converging and trustworthy results. This challenge may emerge particularly when applying an inclusive basis set accommodating diffuse functions[7-12] Consequently, it becomes convenience to identify and apply a method capable of providing all required information derived directly from calculated ground state results of the studied molecular system. For example, one may desire to study a molecular system possible by deriving both the electron affinity (A) and ionization potential (I) without calculating the radical cation and anion. Certainly, such is illustrated by the Koopmans' theorem,[9-12] alleging the possibility of approximating I by subtracting HOMO energy $I = -\varepsilon_H$ within the Hartree-Fock (HF) theory. An extension of this would regard possible approximation of A by subtracting LUMO energy, $A = -\varepsilon_L$.

The validity of using the Koopmans' theorem raises concerns in DFT for overlooking the existence of gaps between the frontier orbital and functional band gaps. Its use then becomes both challenging and controversial for its failure to accommodate and identify differences arising between the HOMO-LUMO and fundamental band gaps. This translates to derivative discontinuity. Recent efforts have proved successful in assigning exact physical meaning in Kohn-Sham (KS) HOMO. This uses the KS analog feature of Koopmans theorem upon the Hartree-Fock theory. Harttree-Fock approach equated KS HOMO to directly matched to the opposite of its ionization potential ($\varepsilon_H = -I$) in exact theory[14-17]. Despite this success, the earlier mentioned derivative discontinuity identified in the Koopmans theorem implies a nonexistence of electron affinity link from the LUMO energy. However, researchers have proposed regard the relation between the anion I and N+1 electron system) derived from a similar relation of A to N electron system. This allows them to overcome the derivative continuity challenge.[13]Kronik et al[13] illustrated that a judicious choice incorporating γ the range-separation parameter could guarantee validity in using the Koopmans theorem. They established that enforcing this validity would require inclusive consideration of range-separated hybrids (RSH) functions, [18-20] however, splitting the repulsive Coulomb potential into short-range and long range terms. This would take a form such as $r^{-1} = r^{-1}\,\mathrm{erf}(\gamma r) + r^{-1}\mathrm{erfc}(\gamma r)$, γ being the range-separation parameter. A careful selection of the last parameter could enforce the validity of Koopmans' theorem.

Applying the γ tuning technique along density functional makes it possible to reinforce the descriptions of properties during predictions. This would realize an advanced fulfillment for the Koopmans' theorem translated to improved validity and agreement within orbital energies and I and A. In particular, Lima et al. [21] demonstrated this possibility by improving descriptions accorded optical properties in carotenoids via tuning the long-range term of corrected functionals.

This implies that the best of a specific density functional is a realizable estimate however, checking how appropriate it complies with the Koopmans' theorem in the DFT. Specifically, checking factors for it to show closer behavior to exact density functional is critical to calculate Conceptual DFT descriptors capable of predicting and explaining chemical reactivity experienced in molecular systems. Nevertheless, the γ tuning approach in RSH density functionals depends on the system. This dependence implies using varying density functional to calculate descriptors relative to the molecular system. Different molecular systems would demand use of different γ tuning procedures. This produces enough reason to examine other RSH density functionals identified with fixed γ parameter through constructions. However, this requires fitting other parameters to regenerate varying molecular properties. Specifically, this will involve considering a number of density functions identified with showing great accuracy amidst broad range of chemistry and physics databases[22].

Flavonoids constitute part of phenolic compounds based on the generic of their chemicals. Their multiple applications and biochemical properties make them an essential category of secondary metabolites. Flavonoids have a similar benzo-γ-pyrone structure identified as a highly ubiquitous compound in plants. Botanical studies acknowledge the discovery of over 4,000 naturally occurring flavoids. They allege unique finding that claims over 36,000 varying chemical structure for a particular flavoids in flavones. This diversity reflects in the wide presence of flavonoids in various edible plants including wine, tea, seed, fruits, grain and vegetables[23].

Several plant flavonoids could be extracted from extract of citrus fruits including Hesperetin (C16H14O6; mol. wt. 302.28 g/mol identified from its IUPAC name as (2S)-5,7-dihydroxy-2-(3-hydroxy-4-methoxyphenyl)-2,3-dihydrochromen-4-one); Neohes-peridin (C28H34O15; mol. wt. 610.56 g/mol known from its IUPAC name as (2S)-7-[(2S,3R,4S,5S,6R)-4,5-dihydroxy-6-(hydroxymethyl)-3-[(3R, 4R, 5R, 6S)-3,4,5-trihydroxy-6-methyloxan-2-yl]oxyoxan-2-yl]oxy-5-hydro- xy-2-(3-hydroxy-4-methoxyphenyl)-2,3-dihydrochromen-4-one) and Hesperidin (C28H34O15; mol. wt. 610.56 g/mol with an IUPAC identity of (2S)-5-hydroxy-2-(3-hydroxy-4-methoxyphenyl)-7-[(2S,3R,4S,5S,6R)-3,4,5-trihydroxy-6-[[(2R, 3R,4R,5R,6S)-3,4,5-trihydroxy-6-methyloxan-2-yl] oxymethyl] oxan-2-yl]oxy-2,3-dihydrochromen-4-one). They are identified as useful antioxidants in resolving the nonenzymatic glycation experienced in amino acids and proteins. They achieve this by complexing metals such as Cu, Al and Fe. This work desires conducting a comparative study examining the performance of recent Minnesota group of density functionals in describing the chemical reactivity of abovementioned flavonoids. Their molecular structures are demonstrated below in Figure-1.

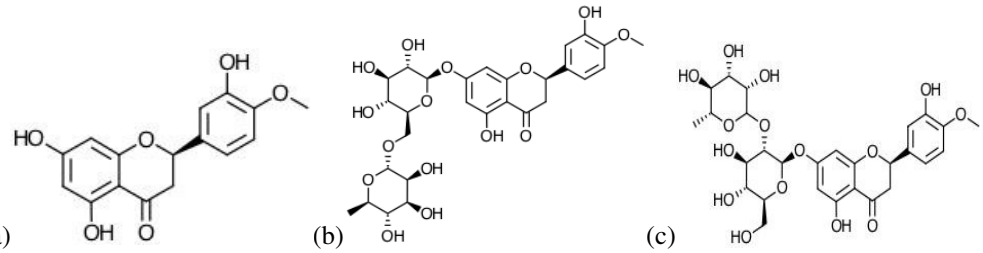

(a) (b) (c)

Figure-1: Molecular Structure of the a) Hesperetin, b) Hesperidin and c) Neohesperidin Flavonoids.

Theoretical background

The chemical potential μ, existing in the conceptual structure of DFT,[2,24] measures the tendency of electron to escape from the equilibrium. This potential is identified as:

$$\mu = \left(\frac{\partial E}{\partial N}\right)_{v(r)} = -\chi \quad (1)$$

χ being the electro negativity index.

The global hardness η is seen as causing resistance to charge transfers defined as:

$$\eta = \left(\frac{\partial^2 E}{\partial N^2}\right)_{v(r)} \quad (2)$$

It is possible to apply a finite variance of approximation linked with the Koopmans' theorem,[9-12] to rewrite the expressions outlined above as:

$$\mu = -\frac{1}{2}(I + A) \approx \frac{1}{2}(\varepsilon_H + \varepsilon_L) = \chi_K \quad (3)$$

$$\eta = (I - A) \approx (\varepsilon_H - \varepsilon_L) = \eta_K \quad (4)$$

ε_H showing the energies of the highest occupied HOMO and ε_L representing energies of the lowest unoccupied orbital of a molecular LUMO. The findings of Perdew and Levy justify the existence of these inequalities in DFT context.[16] They alleged emerging importance of the highest occupied Kohn–Sham eigen values. Besides, they proved the occurrence of ionization potential theorems upon the exact KS DFT derived from a multiple-electron system. Moreover, Janak's Theorem provides further support for the application of frontier molecular orbital energies by approximating them to derive I and A.[25] Specifically, Janak theorem found KS HOMO and negative determining the lower and upper limits respectively to derive experimental values identified as possessing the first ionization potential [26]. This position proves crucial to validate the application of energies drawn from Kohn-Sham frontier in molecular orbital in calculation the chemical reactivity descriptors originating from Conceptual DFT.

The use of electrophilicity index ω shows the resulting stabilization energy witnessed in systems when saturated with electrons originating from the surrounding of the system. This is defined as:

$$\omega = \frac{\mu^2}{2\eta} = \frac{(I+A)^2}{4(I-A)} \approx \frac{(\varepsilon_H+\varepsilon_L)^2}{4(\varepsilon_H-\varepsilon_L)} = \omega_K \quad (5)$$

where electroaccepting (ω^+) and electrodonating (ω^-) powers are determined a[27]:

$$\omega^- = \frac{(3I+A)^2}{16(I-A)} \approx \frac{(3\varepsilon_H+\varepsilon_L)^2}{16\eta_K} = \omega_K^- \quad (6)$$

$$\omega^+ = \frac{(I+3A)^2}{16(I-A)} \approx \frac{(\varepsilon_H+3\varepsilon_L)^2}{16\eta_K} = \omega_K^+ \quad (7)$$

It implies that advanced abilities to accept charge translates to larger ω^+values whereas, better electron donation is shown by smaller ω^-value of the molecular system. From this position, researchers have sought better comparison between $\omega^+$and $-\omega^\pm$ prompting the definition of net electrophilicity proposed as[28]:

$$\Delta\omega^\pm = \omega^+ - (-\omega^-) \approx \omega_K^+ - (-\omega_K^-) = \omega_K^+ + \omega_K^- = \Delta\omega_K^\pm \quad (8)$$

that is, the electroaccepting power relative to the electrodonating power.

The electronic density forms the first local reactivity descriptor in restricted levels applied when electrostatic interactions are dominant between and amidst molecules yet under the Conceptual DFT framework. This is defined as:[1]

$$\rho(r) = \left[\frac{\delta E}{\delta v(r)}\right]_N \quad (9)$$

By contrast, governance of chemical reactions by interactions of covalent form encourage the use of second order LRD identified as fukui function rather than the electronic density.[2] The second order LRD involves derivative ρ(r) obtained with respect to N. This is done using a Maxwell relation by interpreting the same descriptor mainly as a variation of μ relative to υ(r):

$$f(r) = \left(\frac{\partial \rho(r)}{\partial N}\right)_{v(r)} = \left[\frac{\delta \mu}{\delta v(r)}\right]_N \quad (10)$$

The function $f(r)$ is interpreted as reflecting the potential of molecular site in accepting and donating electron. Achieving higher $f(r)$ values demonstrate high reactivity derived at point r.[2]

Considering that electron numbers (N) involves a discrete variable[29] translate to the emergence of right and left derivatives ρ(r) relative to N. Introducing the finite difference approximation in equation 10 generates two Fukui functions relative to the total electronic densities as shown below:

$$f^{+}(r) = \left(\frac{\partial\rho(r)}{\partial N}\right)^{+}_{v(r)} = \rho_{N+1}(r) - \rho_N(r) \quad (11)$$

$$f^{-}(r) = \left(\frac{\partial\rho(r)}{\partial N}\right)^{-}_{v(r)} = \rho_N(r) - \rho_{N-1}(r) \quad (12)$$

with $\rho_{N+1}(r)$, $\rho_N(r)$, and $\rho_{N-1}(r)$showing the electronic densities emerging at point r for the molecular system corresponding to N+1, N and N−1 electrons. The $f^{+}(r)$, emerges from the reactivity obtained for a nucleophilic attack thus calculating the intramolecular reactivity occurring at site *r* to the nucleophilic reagent. The $f^{-}(r)$, links to the reactivity developing from electrophilic attack, thus a function to calculate the intramolecular reactivity experienced at *r* to the electrophilic reagent[24].

Condensing to the function to the atoms necessitated integrating it within the k[th]–atomic domain Ω_k outlined below [30,31]:

$$f_k^{\pm} = \int_{\Omega_k} f^{\pm}(r)dr \quad (13)$$

The function $f_k^{\pm}$ realized an atomic index form fit to define the electrophilic and nucleophilic power in the atom *k*. From this index, Morell et al.[3,32-37] proposed the existence of local reactivity descriptor they named dual descriptor (DD) $f^{(2)}(r) \equiv \Delta f(r)$. They developed its mathematical definition by deriving the Fukui function, $f(r)$,[2] relative to the electron number, N. They obtained $\Delta f(r)$ is shown as: [32,33]

$$\Delta f(r) = \left(\frac{\partial f(r)}{\partial N}\right)_{v(r)} = \left[\frac{\delta\eta}{\delta v(r)}\right]_N \quad (14)$$

Condensing the dual descriptor necessitated using a similar integration factor k[th]–atomic domain Ω_k to obtain:

$$\int_{\Omega_k} \Delta f(r)dr = \Delta f_k \quad (15)$$

Morell et al. held that $\Delta f_k > 0$, illustrated a nucleophilic attack on atom k forcing the atom to act similarly to electrophilic species. By contrast, Δf_k<0, showed electrophilic attacks that made the atom k assume actions of nucleophilic species.

Nevertheless, the dual descriptor shows a subintensive property implying that condensing it makes its values insignificant with increasing molecule size. this stimulated defining a second local reactivity descriptor to address the intrinsic behavior noted in the first. Specifically, this sought enabling the measurement of local reactivities relative to molecular size[34,35], called the local hypersoftness (LHS). They expressed LHS working as:

$$s^{(2)}(r) \approx \frac{\Delta f(r)}{\eta^2} = \Delta f(r) \cdot S^2 \quad (16)$$

with S showing global softness,[1,38,39] being the inverse of global hardness η. They could equally condense LHS by integrating it on basis of the k[th]–atomic domain Ω_k:

$$\int_{\Omega_k} s^{(2)}(r)dr = s_k^{(2)} \quad (17)$$

This definition eased its use by ensuring a comparable measure of local reactivity experienced on the molecular system and that witnessed in other systems regardless of size differences.

Settings and Computational Methods

The settings were done in accordance with the computational package. Gaussian 09[40] programs series were used to perform the computation alongside density functional methods as guided in the computational package. The gradient technique was applied in determining the equilibrium geometries in the molecules. Besides, calculating analytical frequencies was considered to determine the vibrational frequencies and force constants. This was done on stationary points derived after optimizing to affirm their true minima. The use of Def2SVP basis set was important to realize geometry optimizations while Def2TZVP used in calculating electronic properties[41,42].

Choosing a wider range of density functionals was considered to calculate the molecular structure. A similar selection was chosen to calculate the properties existing in the system. The selection of Minnesota density functionals family was considered suitable in both cases considering its satisfactory results in calculating structural and thermodynamic properties[22]. They included M11 in range-separated hybrid meta-GGA[43], M11L dual-range local meta-GGA[44], MN12L, for nonseparable local meta-NGA[45], MN12SX for its separated range and hybrid nonseparable meta-NGA[46], N12 to offer nonseparable gradient approximation[47], supported by N12SX in approximating range-separated and hybrid nonseparable gradient,[46]. Inclusion of SOGGA11 for GGA density functional[48] alongside SOGGA11X in hybrid GGA density functional to allow adequate calculation[49].

GGA in the functions implied generalized gradient approximation a key factor depended on by density function for up and down spins and reducing their gradient. NGA expressed the nonseparable gradient approximation used by density functional in up-down spin densities, their condensed gradient. This was equally adopted in nonseparable form. Water served the source solvent in all calculations. IEF-PCM computations embraces the SMD solvation model[50].

Results and discussion

Gabedit 2.4.8 program provided means to identify the most constant conformer. Prioritizing the available PDB structure

facilitated the pre-optimization of molecular structures.[51] This was done to Hesperetin, Hesperidin and Neohesperidin structures. Random sampling was performed with molecular mechanics techniques and inclusion of all torsional angles. The selected Minnesota family of density functionals allowed re-optimizing structures of emerging conformers; specifically using M11, M11L, MN12L, MN2SX, N12, N12SX, SOGGA11 and SOGGA11X. The preoptimization process was enhanced further using the Def2SVP basis set in conjunction with the SMD solvation model, with water being the solvent.

Earlier discussion showed a controversial Koopmans' theorem for its weak validity within the DFT approximation. It was equally illustrated[26] using KS orbitals generates Conceptual DFT reactivity descriptors found correlating appropriately with reactivity descriptors derived using the Hartree-Fock calculations. This proved crucial despite the distinct from the shape and energy evident in HF. In addition, the verification of procedures for quality was done by calculating the global hardnessη, electronegativity χ, and the global electrophilicityω. The calculation of electrodonatingω^- power and electroaccepting ω^+ power alongside net electrophilicity $\Delta\omega^{\pm}$ ensured further verification of the procedures.

Tables-1, 2 and 3 capture the results from calculations performed on Hesperetin, Hesperidin and Neohesperidin molecules. They capture results of HOMO orbital energies (in eV), LUMO orbital energies (in eV), ionization potentials I in (in eV), electron affinities A (in eV), global electronegativity χ, total hardness η, global electrophilicity ω, electrodonating power ω^-, electroaccepting power ω^+, and net electrophilicity $\Delta\omega^{\pm}$. These are conducted using several density functional including M11, M11L, MN12L, MN12SX, N12, N12SX, SOGGA11, and SOGGA11X. The calculation embraces the Def2TZVP basis set and water solvent. The IEF-PCM model is used to stimulate them with the SMD parametrization. The upper section of the tables captures subscript K illustrating the derivation of results assumed validity in Koopmans theorem in DFT. The lower section demonstrates results obtained by calculating vertical I and A.

Table-1: HOMO and LUMO orbital energies (in eV), ionization potentials I and electron affinities A (in eV), and global electronegativity χ, total hardness η, global electrophilicityω, electrodonating power ω^-, electroaccepting power ω^+, and net electrophilicity $\Delta\omega^{\pm}$of Hesperetin calculated with the M11, M11L, MN12L, MN12SX, N12, N12SX, SOGGA11 and SOGGA11X density functionals and the Def2TZVP basis set using water as solvent simulated with the SMD parametrization of the IEF-PCM model . The upper part of the table shows the results derived assuming the validity of Koopmans' theorem and the lower part shows the results derived from the calculated vertical I and A.

Property	M11	M11L	MN12L	MN12SX	N12	N12SX	SOGGA11	SOGGA11X
HOMO	-8.817	-5.797	-5.628	-6.222	-5.171	-6.019	-5.523	-7.127
LUMO	0.398	-2.058	-1.783	-1.726	-2.077	-1.739	-2.382	-0.867
χ_K	4.210	3.928	3.706	3.974	3.624	3.879	3.952	3.997
η_K	9.215	3.739	3.845	4.496	3.094	4.280	3.141	6.261
ω_K	0.962	2.063	1.786	1.756	2.122	1.757	2.487	1.276
ω_K^-	4.604	6.323	5.664	5.780	6.250	5.722	7.146	4.942
ω_K^+	0.394	2.395	1.959	1.806	2.626	1.843	3.193	0.945
$\Delta\omega_K^{\pm}$	4.998	8.718	7.623	7.587	8.877	7.565	10.339	5.886
I	6.353	5.979	5.797	6.172	5.414	5.965	5.744	6.167
A	1.968	1.866	1.586	1.823	1.690	1.833	1.985	1.809
χ	4.160	3.922	3.691	3.998	3.552	3.899	3.864	3.988
η	4.385	4.113	4.210	4.348	3.725	4.131	3.759	4.358
ω	1.974	1.870	1.618	1.838	1.694	1.840	1.986	1.824
ω^-	6.302	5.959	5.345	5.946	5.396	5.887	6.139	5.915
ω^+	2.141	2.036	1.654	1.948	1.844	1.988	2.275	1.927
$\Delta\omega^{\pm}$	8.443	7.995	6.999	7.894	7.241	7.876	8.414	7.842

Table-2: HOMO and LUMO orbital energies (in eV), ionization potentials I and electron affinities A (in eV), and global electronegativity χ, total hardness η, global electrophilicityω, electrodonating power ω^-, electroaccepting power ω^+, and net electrophilicity $\Delta\omega^\pm$of Hesperidin calculated with the M11, M11L, MN12L, MN12SX, N12, N12SX, SOGGA11 and SOGGA11X density functionals and the Def2TZVP basis set using water as solvent simulated with the SMD parametrization of the IEF-PCM model . The upper part of the table shows the results derived assuming the validity of Koopmans' theorem and the lower part shows the results derived from the calculated vertical I and A.

Property	M11	M11L	MN12L	MN12SX	N12	N12SX	SOGGA11	SOGGA11X
HOMO	-8.510	-5.520	-5.368	-5.963	-4.810	-5.600	-5.132	-6.717
LUMO	0.215	-2.186	-1.949	-1.856	-2.151	-1.778	-2.348	-0.937
χ_K	4.148	3.853	3.659	3.910	3.480	3.689	3.740	3.827
η_K	8.725	3.334	3.419	4.107	2.659	3.822	2.785	5.779
ω_K	0.986	2.227	1.958	1.861	2.277	1.780	2.511	1.267
ω_K^-	4.591	6.588	5.959	5.934	6.461	5.644	7.067	4.809
ω_K^+	0.443	2.735	2.300	2.024	2.981	1.955	3.327	0.982
$\Delta\omega_K^\pm$	5.034	9.323	8.259	7.958	9.441	7.599	10.394	5.791
I	6.113	5.774	5.606	5.924	5.166	5.552	5.423	5.779
A	2.089	1.986	1.749	1.945	1.768	1.864	1.968	1.852
χ	4.101	3.880	3.678	3.935	3.467	3.708	3.695	3.815
η	4.024	3.788	3.857	3.979	3.398	3.688	3.455	3.927
ω	2.090	1.987	1.754	1.945	1.768	1.864	1.976	1.853
ω^-	6.483	6.152	5.587	6.107	5.483	5.812	6.016	5.859
ω^+	2.381	2.271	1.909	2.172	2.016	2.104	2.320	2.044
$\Delta\omega^\pm$	8.864	8.423	7.496	8.279	7.498	7.917	8.336	7.904

Table-3: HOMO and LUMO orbital energies (in eV), ionization potentials I and electron affinities A (in eV), and global electronegativity χ, total hardness η, global electrophilicityω, electrodonating power ω^-, electroaccepting power ω^+, and net electrophilicity $\Delta\omega^\pm$of Neohesperidin calculated with the M11, M11L, MN12L, MN12SX, N12, N12SX, SOGGA11 and SOGGA11X density functionals and the Def2TZVP basis set using water as solvent simulated with the SMD parametrization of the IEF-PCM model . The upper part of the table shows the results derived assuming the validity of Koopmans' theorem and the lower part shows the results derived from the calculated vertical I and A.

Property	M11	M11L	MN12L	MN12SX	N12	N12SX	SOGGA11	SOGGA11X
HOMO	-8.405	-5.414	-5.246	-5.844	-4.896	-5.658	-5.103	-6.737
LUMO	0.223	-2.179	-2.019	-1.815	-2.154	-1.803	-2.425	-0.967
χ_K	4.091	3.797	3.632	3.830	3.525	3.730	3.764	3.852
η_K	8.629	3.235	3.227	4.029	2.742	3.855	2.678	5.770
ω_K	0.970	2.227	2.045	1.820	2.265	1.805	2.645	1.286
ω_K^-	4.525	6.555	6.107	5.807	6.464	5.716	7.340	4.859
ω_K^+	0.433	2.759	2.475	1.977	2.939	1.986	3.576	1.006
$\Delta\omega_K^\pm$	4.958	9.314	8.582	7.783	9.403	7.702	10.916	5.865
I	6.009	5.679	5.513	5.798	5.217	5.612	5.402	5.807
A	2.102	1.966	1.811	1.907	1.755	1.889	1.988	1.894
χ	4.056	3.823	3.662	3.853	3.486	3.751	3.695	3.850
η	3.907	3.713	3.701	3.891	3.463	3.723	3.414	3.913
ω	2.105	1.968	1.812	1.908	1.755	1.889	1.999	1.894
ω^-	6.483	6.080	5.686	5.985	5.469	5.887	6.059	5.958
ω^+	2.427	2.257	2.024	2.132	1.983	2.136	2.364	2.108
$\Delta\omega^\pm$	8.910	8.337	7.709	8.117	7.452	8.023	8.424	8.065

The design of several descriptors emerged from previous tasks on similar DFT subject[13,21] and desire to analyze the results obtained objectively to ascertain whether Koopmans' theorem in DFT was fulfilled. For this reason, the descriptors designed desire to relate results derived by performing HOMO and LUMO calculations and those generated by calculating vertical I and A using ΔSCF procedure. This design does not seek performing gap-fitting procedures to minimize the descriptors through optimal choices of range-separation parameter γ. Rather, it seeks to check whether density functionals used in this study comply with the Koopmans' theorem in DFT. This is necessary since some are having fixed range-separation parameter γ. Indeed, range-separation parameter γ is excluded in the design of these descriptors. The design treats A as representing the minus energy in LUMO of a neutralized system rather than as minus the energy of the HOMO in the N+1 electron system[13,21].

The initial three descriptors show a simple fulfillment of Koopmans' theorem linking ε_H with -I, ε_L with -A, and their collective behavior in the HOMO-LUMO gap description:

$$J_I = \left|\epsilon_H + E_{gs}(N-1) - E_{gs}(N)\right| \quad (18)$$

$$J_A = \left|\epsilon_L + E_{gs}(N) - E_{gs}(N+1)\right| \quad (19)$$

$$J_{HL} = \sqrt{J_I^2 + J_A^2} \quad (20)$$

Four descriptors are subsequently considered in analyzing how well the density functional studies become useful in predicting global hardness η, global electrophilicityω and electronegativity χ along with combined Conceptual DFT descriptors adopting comparable energies in HOMO and LUMO and the vertical I and A:

$$J_\chi = |\chi - \chi_K| \quad (21)$$

$$J_\eta = |\eta - \eta_K| \quad (22)$$

$$J_\omega = |\omega - \omega_K| \quad (23)$$

$$J_{D1} = \sqrt{J_\chi^2 + J_\eta^2 + J_\omega^2} \quad (24)$$

Lastly, another set of four descriptors is designed to verify goodness present in density functional studied in predicting electroaccepting power ω^+, electrodonating power ω^-, and net electrophilicity $\Delta\omega^\pm$, alongside combined conceptual DFT descriptors, relative to energies of either vertical I and A or HOMO and LUMO:

$$J_{\omega^+} = |\omega^+ - \omega_K^+| \quad (25)$$

$$J_{\omega^-} = |\omega^- - \omega_K^-| \quad (26)$$

$$J_{\Delta\omega^\pm} = |\Delta\omega^\pm - \Delta\omega_K^\pm| \quad (27)$$

$$J_{D2} = \sqrt{J_{\omega^+}^2 + J_{\omega^-}^2 + J_{\Delta\omega^\pm}^2} \quad (28)$$

D2 representing the second category of Conceptual DFT descriptors. Tables 4, 5, and 6, display results obtained by calculating J_I, J_A, J_{HL}, J_χ, J_η, J_ω, J_{D1}, J_{ω^+}, J_{ω^-}, $J_{\Delta\omega^\pm}$and J_{D2} for each Hesperetin, Hesperidin and Neohesperidin molecules.

Table-4: Descriptors J_I, J_A, J_{HL}, J_χ, J_η, J_ω, J_{D1}, J_{ω^+}, J_{ω^-}, $J_{\Delta\omega^\pm}$*and* $J_{D2}$for the Hesperetin molecule calculated from the results of Table 1.

Descriptor	M11	M11L	MN12L	MN12SX	N12	N12SX	SOGGA11	SOGGA11X
J_I	2.465	0.182	0.169	0.050	0.244	0.054	0.221	0.960
J_A	2.366	0.192	0.197	0.098	0.387	0.095	0.397	0.942
J_{HL}	3.416	0.264	0.259	0.110	0.458	0.109	0.454	1.345
J_χ	0.049	0.005	0.014	0.024	0.072	0.020	0.088	0.009
J_χ	4.830	0.374	0.366	0.148	0.631	0.149	0.618	1.902
J_χ	1.012	0.192	0.167	0.082	0.429	0.082	0.501	0.548
J_{D1}	4.936	0.420	0.402	0.171	0.766	0.171	0.800	1.980
J_{ω^+}	1.698	0.364	0.319	0.166	0.854	0.166	1.007	0.973
J_{ω^-}	1.747	0.359	0.305	0.142	0.782	0.145	0.918	0.983
$J_{\Delta\omega^\pm}$	3.445	0.723	0.624	0.308	1.636	0.311	1.925	1.956
J_{D2}	4.219	0.886	0.765	0.377	2.005	0.382	2.358	2.395

Table-5: Descriptors J_I, J_A, J_{HL}, J_χ, J_η, J_ω, J_{D1}, J_{ω^+}, J_{ω^-}, $J_{\Delta\omega^\pm}$ *and* J_{D2} for the Hesperidin molecule calculated from the results of Table 2.

Descriptor	M11	M11L	MN12L	MN12SX	N12	N12SX	SOGGA11	SOGGA11X
J_I	2.397	0.254	0.238	0.039	0.356	0.048	0.290	0.938
J_A	2.304	0.200	0.200	0.089	0.383	0.086	0.380	0.914
J_{HL}	3.325	0.323	0.311	0.097	0.523	0.098	0.478	1.310
J_χ	0.046	0.027	0.019	0.025	0.013	0.019	0.045	0.012
J_χ	4.701	0.454	0.438	0.128	0.739	0.133	0.670	1.852
J_χ	1.104	0.239	0.204	0.084	0.509	0.084	0.535	0.586
J_{D1}	4.829	0.514	0.483	0.155	0.897	0.159	0.859	1.943
J_{ω^+}	1.892	0.437	0.372	0.173	0.978	0.168	1.051	1.050
J_{ω^-}	1.938	0.464	0.391	0.148	0.965	0.149	1.007	1.062
$J_{\Delta\omega^\pm}$	3.830	0.900	0.763	0.321	1.943	0.318	2.058	2.113
J_{D2}	4.691	1.103	0.934	0.394	2.380	0.389	2.520	2.588

Table-6: Descriptors J_I, J_A, J_{HL}, J_χ, J_η, J_ω, J_{D1}, J_{ω^+}, J_{ω^-}, $J_{\Delta\omega^\pm}$ *and* J_{D2} for the Neohesperidin molecule calculated from the results of Table 3.

Descriptor	M11	M11L	MN12L	MN12SX	N12	N12SX	SOGGA11	SOGGA11X
J_I	2.396	0.265	0.267	0.046	0.321	0.046	0.299	0.931
J_A	2.326	0.212	0.208	0.092	0.399	0.086	0.437	0.926
J_{HL}	3.339	0.339	0.338	0.103	0.512	0.098	0.530	1.313
J_χ	0.035	0.026	0.030	0.023	0.039	0.020	0.069	0.002
J_χ	4.722	0.477	0.475	0.139	0.720	0.132	0.736	1.857
J_χ	1.135	0.259	0.233	0.088	0.510	0.084	0.646	0.608
J_{D1}	4.857	0.544	0.530	0.166	0.884	0.158	0.982	1.954
J_{ω^+}	1.958	0.476	0.421	0.178	0.995	0.171	1.281	1.009
J_{ω^-}	1.993	0.502	0.451	0.155	0.956	0.150	1.212	1.101
$J_{\Delta\omega^\pm}$	3.952	0.978	0.872	0.333	1.952	0.321	2.492	2.200
J_{D2}	4.840	1.198	1.069	0.409	2.390	0.393	3.053	2.695

Comparing the Tables-1, 2 and 3 results with their corresponding results displayed in Tables-4, 5 and 6, shows satisfaction of Koopmans' theorem accurately for MN12SX and N12SX density functional considered range-separated hybrid meta-NGA and a range-separated hybrid NGA respectively. Certainly, their values derived for JI, $J_A$andJ_{HL} do not reflect exact zero. Nevertheless, these values feature favorable comparison with results attained in similar quantities observed by Lima et al[21]. They reveal a minimum achieved through selection of parameters enforcing such behavior.

Interestingly, the same density functionals display satisfaction of Koopmans' theorem in DFT for descriptors J_{χ}, J_{η}, J, and J_{D1}, along with $J_{\omega}-$, $J_{\omega}+$, $J_{\Delta\omega}\pm$, and J_{D2}. This shows the importance of results obtained for showing that J_I, J_A and J_{HL} are not exhaustive to rely on. For instance, J_{χ}, shows values of closest to zero for all density functionals tested. MN12SX and N12SX are the only descriptors showing a similar behavior for density functionals. The results obtained for J_{χ}reveal possible explanation for a casual cancellation of errors. Moreover, GGA (SOGGA11) and hybrid-GGA (SOGGA11X) suggest they are neither good enough to fulfill the Koopmans' theorem in DFT, a conclusion similarly valid in the local functionals M11L, MN12L and N12.

The results show consistency, perhaps factual that though the range-separated hybrid NGA and range-separated hybrid meta-NGA density functionals prove capability for calculating the Conceptual DFT descriptors, they demonstrate a converse for the range- separated hybrid GGA (M11) density functional. Further examination of Tables-1 to 3 reveal that the functionals describe the LUMOs energy inadequately translated to the negative values obtained for A thereby contradicting the ΔSCF results.

The reactivity of each atom in the molecular system can be determined by using the condensed Fukui functions. Using the corresponding condensed functions namely $f_k^+ = q_k(N+1) - q_k(N)$, $f_k^- = q_k(N) - q_k(N-1)$, and $f_k^0 = {}^1/_2\,[q_k(N+1) - q_k(N-1)$ for nucleophilic attack, electrophilicattack and radical attack respectively q_k being the gross charge of each atom k in the molecular system.

This becomes possible to examine the condensed Fukui functions using single-points calculations directly unlike other verification requiring additional calculations. This is demonstrated as following for N-1 and N+1 electrons:

$$f_k^+ = \sum_{a\in k}[c_{ai}^2 + c_{ai}\sum_{b\neq a} c_{bi}S_{ab}] \quad (29)$$

i being LUMO, and

$$f_k^- = \sum_{a\in k}[c_{ai}^2 + c_{ai}\sum_{b\neq a} c_{bi}S_{ab}] \quad (30)$$

i being HOMO, withc_{ai}being the LCAO coefficients and S_{ab} the overlap matrix. The condensed Fukui functions are normalized, thus $\sum_k f_k = 1$ and $f_k^0 = {}^1/_2\,[f_k^+ + f_k^-]$.

Using the interpretation earlier outlined for Fukui functions, the sign seen in the dual descriptor is very useful in characterizing the site reactivity within the molecular system. This determines the nature of the reactivity whether towards a nucleophilic or electrophilic attack. Where $\Delta f_k > 0$, this suggests the site favors a nucleophilic attack unlike an electrophilic attack if $\Delta f_k < 0$.[32,33,54]

Table-7 shows results of the condensed dual descriptor Δf_k performed on atoms of Hesperetin molecule. A similar selection of density functionals (from M11 to SOGGA11X) is used in calculating coupled by Def2TZVP basis set. SMD parametrization approach of the IEF-PCM model is used in simulating water used as the solvent.

Analysis of Table-7 demonstrate that density functional considered here imply CII as the preferred site for the nucleophilic attack. This shows the carbonyl carbon, meaning that repeat calculations performed for Hesperidin and Neohesperidin molecules show C atom being the preferred site for nucleophilic attack.

This observation changes with the molecular size. This makes it impossible to compare directly the condensed dual descriptor Δf_kacross the atoms. This obligated calculation of respective value for condensed local hypersoftness $s_k^{(2)}$on carbonyl C atoms k for the Hesperetin, Hesperedin and Neohesperidin molecules based on the accuracy attained for MN12SX and N12SX density functionals. Atomic units were used to express Δf_k and S measured using mili eV^{-1}. Conversion of mili eV^{-1} factor is done to 10^{-3} and S raised to power of 2 prior to the multiplication. The value obtained utilizes milieV unit raised to power of -2 m(eV^{-2}). The inclusion of this parenthesis clarifies the exclusion of prefix mili from the power of -2.

The results obtained for the MN12SX density functional showed 13.169 m(eV^{-2}) for Hesperetin, Hesperidin at 14.152 m(eV^{-2}) and 15.777 m(eV^{-2}) for Neohesperidin. The N12SX density functional showed 14.685 m(eV^{-2}) for Hesperetin, Hesperidin at 18.216 m(eV^{-2}) and 17.569 m(eV^{-2}) for the Neohesperidin. This confirmed that the chemical reactivity experienced of the carbonyl C corresponds to the nucleophilic attack site marked by a similar trend of Hesperetin<Neohesperidin< Hesperidin.

It can be concluded from the analysis of the results on Table-7 that all density functionals considered in this study predict that C11 will be the preferred site for a nucleophilic attack. This the carbonyl carbon and, if we repeat the calculations for the Hesperidin and Neohesperidin molecules, it is also found that this C atom will be the preferred site for the nucleophilic attack. However, as the size of the molecules is different, the condensed dual descriptor Δf_kover those atoms cannot be directly compared. Thus, we have calculated the corresponding condensed local hypersoftness$s_k^{(2)}$over the carbonyl C atoms of k the three molecules based on the shown accuracy of the MN12SX and N12SX density functionals. It must be stressed that $\Delta f_k$is expressed in atomic units, while S is measured in mili eV raised to the power of -1, however before performing the multiplication, the mili factor is turned back into $10^{-3}$and then S is raised to the power of 2; the resulting value uses the unit milieV raised to the power of -2, meaning m(eV^{-2}); the parenthesis is put in order to make clear that the prefix mili is not raised to the power of -2.

Table-7: Condensed dual descriptor Δf_k over the atoms of the Hesperetin molecule calculated with the M11, M11L, MN12L, MN12SX, N12, N12SX, SOGGA11 and SOGGA11X density functionals and the Def2TZVP basis set using water as solvent simulated with the SMD parametrization of the IEF-PCM model. H atoms are not shown.

Atom	M11	M11L	MN12L	MN12SX	N12	N12SX	SOGGA11	SOGGA11X
1 O	-0.001	-0.004	0.000	0.001	0.000	0.004	-0.014	0.007
2 O	0.133	0.122	0.138	0.142	0.135	0.143	0.072	0.134
3 O	0.014	0.012	0.017	0.016	0.021	0.019	0.010	0.017
4 O	-0.038	-0.029	-0.038	-0.033	-0.075	-0.053	-0.032	-0.036
5 O	-0.122	-0.130	-0.142	-0.129	-0.127	-0.131	-0.122	-0.127
6 O	0.025	0.032	0.032	0.028	0.036	0.031	0.037	0.027
7 C	0.015	0.012	0.013	0.013	0.005	0.009	0.008	0.013
8 C	-0.005	-0.008	-0.007	-0.005	-0.008	-0.002	-0.021	0.000
9 C	-0.113	-0.080	-0.089	-0.100	-0.095	-0.104	-0.071	-0.106
10 C	0.063	0.044	0.048	0.052	0.041	0.053	0.037	0.059
11 C	0.262	0.266	0.264	0.266	0.275	0.269	0.257	0.262
12 C	0.095	0.088	0.089	0.093	0.089	0.093	0.077	0.096
13 C	-0.023	-0.027	-0.030	-0.030	-0.018	-0.027	-0.018	-0.032
14 C	-0.209	-0.203	-0.208	-0.220	-0.174	-0.203	-0.147	-0.227
15 C	0.100	0.096	0.099	0.102	0.099	0.103	0.086	0.106
16 C	0.004	-0.015	0.000	0.002	-0.001	0.007	-0.026	0.012
17 C	-0.173	-0.150	-0.158	-0.176	-0.147	-0.173	-0.108	-0.187
18 C	-0.001	-0.019	-0.006	-0.002	-0.006	0.002	-0.037	0.009
19 C	0.155	0.142	0.140	0.147	0.137	0.146	0.130	0.154
20 C	-0.005	-0.001	-0.005	-0.006	-0.011	-0.008	-0.004	-0.007
21 C	-0.187	-0.170	-0.175	-0.182	-0.177	-0.185	-0.131	-0.187
22 C	-0.006	-0.007	-0.007	-0.006	-0.008	-0.008	-0.008	-0.007

The results for the MN12SX density functional are: Hesperetin: 13.169 m(eV^{-2}), Hesperidin: 14.152 m(eV^{-2}) and Neohesperidin: 15.777 m(eV^{-2}). For the case of the N12SX density functional, the results are: Hesperetin: 14.685 m(eV^{-2}), Hesperidin: 18.216 m(eV^{-2}) and Neohesperidin: 17.569 m(eV^{-2}). Thus, the chemical reactivity of the carbonyl C as the site for the nucleophilic attack will follow the trend: Hesperidin >Neohesperidin>Hesperetin.

Conclusion

The study involves a comparison performed on the Minnesota family density functionals in calculating Conceptual DFT descriptors on citrus flavonoids. Specifically, the study aims at assessing their usefulness in computing the properties and structure of three molecules potentially inhibitors of the nonenzymatic glycation of amino acids and proteins. Choosing

the models to study the molecular system and intended chemical reactions, a process achieved initially prior to using the Conceptual DFT in calculating the chemical reactivity descriptors and active sites. Here, a clear build up to the model is emphasized to ensure validity in the model. A detailed build up is observed by designing several descriptors to verify the fulfillment of the Koopmans' theorem in DFT whose calculated results of HOMO and LUMO compared by means of the vertical I and A with a ΔSCF procedure.

The Kohn-Sham theory is applied to generate values for the Conceptual DFT Descriptors and supports calculations for frontier orbital energies - HOMO and LUMO. Applying the γ tuning technique along density functional makes it possible to reinforce the descriptions of properties during predictions. This achieves advanced fulfillment for the Koopmans' theorem translated to improved validity and agreement within orbital energies and I and A. The study seeks to establish whether the density functionals used obey the Koopmans' theorem in DFT rather than gap-fitting undertaken through the minimization of a descriptor via the choice of the ideal range-separation parameter γ. The use of electrophilicity index ω shows the resulting stabilization energy when saturated with electrons shown through the calculation of where electronegativity χ in addition to the global electrophilicityω together with the global hardness η, electroacceptingω^{+}, electrodonatingω^{-} and net electrophilicity $\Delta\omega^{\pm}$. The condensed Fukui functions, Δf_k is employed to determine the reactivity of each atom in the molecule, whether a nucleophilic attack if $\Delta f_k > 0$, or electrophilic attack if $\Delta f_k < 0$.

The results of this study shows clear capability to predict interaction sites of Hesperetin, Hesperidin and Neohesperidin molecules using DFT-based reactivity descriptors including electronegativity, global electrophilicity, global hardness, electroacceptingand electrodonatingpowers,, and net electrophilicity. Furthermore, Fukui function, condensed dual descriptor and condensed local hypersoftness show consistency in predicting the site. The studies descriptors applied characterization and complete description to demonstrate the preferred reactive sites to generate firm explanations for the chemical reactivities of Hesperetin, Hesperidin and Neohesperidin molecules.

The study tested a Minnesota group of density functionals on whether they accomplish the Koopmans' theorem in DFT through comparison of HOMO- and LUMO- generated values against those derived through the ΔSCF procedure. As per the results, the range-separated, hybrid MN12SX as well as the range-separated, hybrid N12SX optimally meet the objective being tested. Consequently, they confirm as a good alternative to use in place of density functionals reported to showing tuned signs through gap-fitting procedure. This illustrates their usefulness in describing chemical reactivity of large-sized molecular systems.

Acknowledgement

This work has been partially supported by CIMAV, SC and Consejo Nacional de Ciencia y Tecnología (CONACYT, Mexico) through Grant 219566/2014 for Basic Science Research and Grant 265217/2016 for a Foreign Sabbatical Leave. Daniel Glossman-Mitnik conducted this work while a Sabbatical Fellow at the University of the Balearic Islands from which support is gratefully acknowledged. This work was cofunded by the Ministerio de Economía y Competitividad (MINECO) and the European Fund for Regional Development (FEDER) (CTQ2014-55835-R).

References

1. Parr R. and Yang W. (1989). Density-Functional Theory of Atoms and Molecules. Oxford University Press, New York.

2. Geerlings P., Proft De F. and Langenaeker W. (2003). Conceptual Density Functional Theory. *Chemical Reviews*, 103(5), 1793-1873.

3. Torrent-Sucarrat M., Blancafort L., Duran M., Luis J.M. and Solà M. (2007). Theoretical Aspects of Chemical Reactivity. Elsevier Science, Amsterdam, 19, 31.

4. Chattaraj P. (2009). Chemical Reactivity Theory - A Density Functional View. CRC Press. Taylor & Francis Group, Boca Raton.

5. Politzer P. and Murray J. (2002). The Fundamental Nature and Role of the Electrostatic Potential in Atoms and Molecules. *Theoretical Chemistry Accounts,* 108(3), 134-142.

6. Murray J. and Politzer P. (2011). The Electrostatic Potential: An Overview. *WIREs Computational Molecular Science*, 1(2), 153-163.

7. Huzinaga S., Andzelm J., Klobukowski M., Radzio-Audzelm E. (1984). Sakai; Y.; Tatewaki, H. Gaussian Basis Sets for Molecular Calculations, Elsevier, Amsterdam.

8. Easton R., Giesen D., Welch A., Cramer C. and Truhlar D. (1996). The MIDI! Basis Set for Quantum Mechanical Calculations of Molecular Geometries and Partial Charges. *Theoretical Chemistry Accounts,* 93(5), 281-301.

9. Lewars E. (2016). Computational Chemistry - Introduction to the Theory and Ap- plications of Molecular and Quantum Mechanics. Kluwer Academic Publishers, Dordrecht, 2003.

10. Young D. (2001). Computational Chemistry - A Practical Guide for Applying Techniques to Real-World Problems. John Wiley & Sons, New York.

11. Jensen F. (2007). Introduction to Computational Chemistry. 2nd Edition, John Wiley & Sons, Chichester, England.

12. Cramer C. (2013). Essentials of Computational Chemistry - Theories and Models. 2nd Edition, John Wiley & Sons,

Chichester, England.

13. Kronik L., Stein T., Refaely-Abramson S. and Baer R. (2012). Excitation Gaps of Finite-Sized Systems from Optimally Tuned Range-Separated Hybrid Functionals. *Journal of Chemical Theory and Computation*, 8(5), 1515-1531.

14. Perdew J., Parr R., Levy M. and Balduz L.J. (1982). Density-Functional Theory for Fractional Particle Number: Derivative Discontinuities of the Energy. *Physical Review Letters*, 49(23), 1691-1694.

15. Almbladh C.O. and Barth von U. (1985). Exact Results for the Charge and Spin Densities, Exchange-Correlation Potentials, and Density-Functional Eigenvalues. *Physical Review B*., 31(6), 3231-3244.

16. Perdew J., Burke K. and Ersernhof M. (1996). Generalized Gradient Approximation Made Simple. *Physical Review Letters*, 77(18), 3865.

17. Levy M., Perdew J.P. and Sahni V. (1984). Exact Differential Equation for the Density and Ionization Energy of a Many-Particle System. *Physical Review A*, 30(5), 2745-2748.

18. Savin A. (2011). Beyond the Kohn - Sham Determinant. *Recent Advances in Density Functional Methods*, World Scientific, Ch. 4, 129-153.

19. Leininger T., Stoll H., Werner H.-J., Savin A. (1997). Combining Long-Range Configuration Interaction with Short-Range Density Functionals. *Chemical Physics Letters*, 275(3-4), 151-160.

20. Savin A. and Flad H.J. (1995). Density Functionals for the Yukawa Electron-Electron Interaction. *International Journal of Quantum Chemistry,* 56(4), 327-332.

21. Lima I.T., Prado A.d.S., Martins J.B.L., Neto de Oliveira P.H., Ceschin A.M., Cunha da W.F. and Silva Filho da D.A. (2016). Improving the Description of the Optical Properties of Carotenoids by Tuning the Long-Range Corrected Functionals. *The Journal of Physical Chemistry A*, 120(27), 4944-4950.

22. Peverati R. and Truhlar D.G. (2014). Quest for a Universal Density Functional: The Accuracy of Density Functionals Across a Broad Spectrum of Databases in Chemistry and Physics. Philosophical Transactions. Series A, Mathematical, Physical, and Engineering Sciences, 372, 20120476.

23. Marín F., Frutos M., Pérez-Alvarez J., Martinez-Sánchez F. and Río J.D. (2002). Flavonoids as Nutraceuticals: Structural Related Antioxidant Properties and Their Role on Ascorbic Acid Preservation. in: A. Rahman (Ed.), Bioactive Natural Products, Vol. 26, Part G of *Studies in Natural Products Chemistry*, 26, 741-778.

24. Parr R. and Yang W. (1984) Density Functional Approach to the Frontier-Electron Theory of Chemical Reactivity. *Journal of the American Chemical Society*, 106(14), 4049-4050.

25. Janak J. (1978). Proof that $\partial E/\partial n_i = \varepsilon$ in Density Functional Theory. *Physical Review B*, 18(12), 7165-7168.

26. Zevallos J. and Toro-Labbé A. (2003). A Theoretical Analysis of the Kohn-Sham and Hartree-Fock Orbitals and their Use in the Determination of Electronic Properties. *Journal of the Chilean Chemical Society*, 48(4), 39-47.

27. Gázquez J., Cedillo A. and Vela A. (2007). Electrodonating and Electroaccepting Powers. *Journal of Physical Chemistry A*, 111(10), 1966-1970.

28. Chattaraj P., Chakraborty A. and Giri S. (2009). Net Electrophilicity. *Journal of Physical Chemistry A,* 113 (37), 10068-10074.

29. Ayers P. (2008). The Dependence on and Continuity of the Energy and other Molecular Properties with respect to the Number of Electrons. *Journal of Mathematical Chemistry,* 43, 285-303.

30. Fuentealba P., Pérez P. and Contreras R. (2000). On the Condensed Fukui Function. *Journal of Chemical Physics*, 113(7), 2544-2551.

31. Bulat F., Chamorro R., Fuentealba P. and Toro-Labbé A. (2004). Condensation of Frontier Molecular Orbital Fukui Functions. *Journal of Physical Chemistry A*, 108(2), 342-349.

32. Morell C., Grand A. and Toro-Labbé A. (2005). New Dual Descriptor for Chemical Reactivity. *Journal of Physical Chemistry A*, 109, 205-212.

33. Morell C., Grand A. and Toro-Labbé A. (2006). Theoretical Support for Using the Δf(r) Descriptor. *Chemical Physics Letters,* 425(4), 342-346.

34. Cárdenas C., Rabi N., Ayers P., Morell C., Jaramillo P. and Fuentealba P. (2009). Chemical Reactivity Descriptors for Ambiphilic Reagents: Dual Descriptor, Local Hypersoftness, and Electrostatic Potential. *Journal of Physical Chemistry A*, 113(30), 8660-8667.

35. Ayers P., Morell C., De Proft F., Geerlings P. (2007). Understanding the Woodward-Hoffmann Rules by Using Changes in Electron Density. *Chemistry - A European Journal,* 13(29), 8240-8247.

36. Morell C., Ayers P., Grand A., Gutiérrez-Oliva S. and Toro-Labbé A. (2008). Rationalization of the Diels-Alder Reactions through the Use of the Dual Reactivity Descriptor Δf(r). *Physical Chemistry Chemical Physics*, 10(48), 7239-7246.

37. Morell C., Hocquet A., Grand A. and Jamart-Gregoire B. (2008). A Conceptual DFT Study of Hydrazino Peptides: Assessment of the Nucleophilicity of the Nitrogen Atoms by Means of the Dual Descriptor Δf (r). *Journal of Molecular Structure:THEOCHEM*, 849, 46-51.

38. Pearson R. (1993). The Principle of Maximum Hardness. *Accounts of Chemical Research,* 26(5), 250-255.

39. Chermette H. (1999). Chemical Reactivity Indexes in Density Functional Theory. *Journal of Computational Chemistry,* 20, 129-154.

40. Frisch M.J., Trucks G.W., Schlegel H.B., Scuseria G.E., Robb M.A., Cheeseman J.R., Scalmani G., Barone V., Mennucci B., Peters-son G.A., Nakatsuji H., Caricato M., Li X., Hratchian H.P., Izmaylov A.F., Bloino J., Zheng G., Sonnenberg J.L., Hada M., Ehara M., Toyota K., Fukuda R., Hasegawa J., Ishida M., Nakajima T., Honda Y., Kitao O., Nakai H., Vreven T., Montgomery J.A., Peralta J.E., Ogliaro F., Bearpark M., Heyd J.J., Brothers E., Kudin K.N., Staroverov V.N., Kobayashi R., Normand J., Raghavachari K., Rendell A., Burant J.C., Iyengar S.S., Tomasi J., Cossi M., Rega N., Millam J.M., Klene M., Knox J.E., Cross J.B., Bakken V., Adamo C., Jaramillo J., Gomperts R., Stratmann R.E., Yazyev O., Austin A.J., Cammi R., Pomelli C., Ochterski J.W., Martin R.L., Morokuma K., Zakrzewski V.G., Voth G.A., Salvador P., Dannenberg J.J., Dapprich S., Daniels A.D., Farkas O., Foresman J.B., Ortiz J.V., Cioslowski J. and Fox D.J. (2008). Gaussian 09 Revision D.01, Gaussian Inc., Wallingford CT, 2009. *Theor. Chem. Acc,* 120, 215.

41. Weigend F. and Ahlrichs R. (2005). Balanced Basis Sets of Split Valence, Triple Zeta Valence and Quadruple Zeta Valence Quality for H to Rn: Design and Assessment of Accuracy. *Physical Chemistry Chemical Physics*, 7(18), 3297-3305.

42. Weigend F. (2006). Accurate Coulomb-fitting Basis Sets for H to Rn. *Physical Chemistry Chemical Physics*, 8(9), 1057-1065.

43. Peverati R. and Truhlar D.G. (2011). Improving the Accuracy of Hybrid Meta-GGA Density Functionals by Range Separation. *The Journal of Physical Chemistry Letters*, 2(21), 2810-2817.

44. Peverati R. and Truhlar D.G. (2012). M11-L: A Local Density Functional That Provides Improved Accuracy for Electronic Structure Calculations in Chemistry and Physics. *The Journal of Physical Chemistry Letters*, 3(1), 117-124.

45. Peverati R. and Truhlar D.G. (2012). An Improved and Broadly Accurate Local Approximation to the Exchange-Correlation Density Functional: the MN12-L Functional for Electronic Structure Calculations in Chemistry and Physics. *Physical Chemistry Chemical Physics*, 14(38), 13171-13174.

46. Peverati R. and Truhlar D.G. (2012). Screened-Exchange Density Functionals with Broad Accuracy for Chemistry and Solid-State Physics. *Physical Chemistry Chemical Physics*, 14(47), 16187-16191.

47. Peverati R. and Truhlar D.G. (2012). Exchange-Correlation Functional with Good Accuracy for Both Structural and Energetic Properties while Depending Only on the Density and Its Gradient. *Journal of Chemical Theory and Computation*, 8(7), 2310-2319.

48. Peverati R., Zhao Y. and Truhlar D.G. (2011). Generalized Gradient Approximation That Recovers the Second-Order Density-Gradient Expansion with Optimized Across-the-Board Performance. *The Journal of Physical Chemistry Letters*, 2(16), 1991-1997.

49. Peverati R. and Truhlar D.G. (2011). Communication: A Global Hybrid Generalized Gradient Approximation to the Exchange-Correlation Functional That Satisfies the Second-Order Density-Gradient Constraint and Has Broad Applicability in Chemistry. *The Journal of Chemical Physics*, 135(19), 191102.

50. Marenich A., Cramer C. and Truhlar D. (2009). Universal Solvation Model Based on Solute Electron Density and a Continuum Model of the Solvent Defined by the Bulk Dielectric Constant and Atomic Surface Tensions. *Journal of Physical Chemistry B*, 113(18), 6378-6396.

51. Allouche A. (2011). Gabedit – A Graphical User Interface for Computational Chemistry Softwares. *Journal of Computational Chemistry,* 32(1), 174-182.

52. Gorelsky S. (2011). AOMix Program for Molecular Orbital Analysis - Version 6.5, university of Ottawa, Ottawa, Canada (2011).

53. Gorelsky S. and Lever A. (2001). Electronic Structure and Spectra of Ruthenium Di-imine Complexes by Density Functional Theory and INDO/S - Comparison of the Two Methods. *Journal of Organometallic Chemistry*, 635(1-2), 187-196.

54. Gázquez J.L. (2009). Chemical Reactivity Concepts in Density Functional Theory. in: P. K. Chattaraj (Ed.), Chemical Reactivity Theory: A Density Functional View, CRC Press - Taylor & Francis Group, Boca Raton, Fl., 2009, Ch. 2, 7-21.